

(C₆H₅)₅C₆₀H at Si(111)-(7×7) and Ag:Si(111)-(√3×√3)R30° surfacesM. A. Phillips,¹ J. N. O'Shea,¹ P. R. Birkett,² J. Purton,³ H. W. Kroto,⁴ D. R. M. Walton,⁴ R. Taylor,⁴ and P. Moriarty¹¹*The School of Physics and Astronomy, The University of Nottingham, Nottingham NG7 2RD, UK*²*Department of Chemistry and Materials, Manchester Metropolitan University, Manchester M15 6BH, UK*³*Daresbury Laboratory, Warrington WA4 4AD, UK*⁴*Fullerene Science Centre, The University of Sussex, Brighton BN1 9RH, UK*

(Received 29 April 2005; published 16 August 2005)

We have studied the properties of (C₆H₅)₅C₆₀H in thick film form and adsorbed at two surfaces at the extremes of chemical reactivity—the highly reactive Si(111)-(7×7) and chemically passivated Ag:Si(111)-(√3×√3)R30° surfaces—using photoemission spectroscopy (PES) and near-edge x-ray fine structure (NEXAFS) spectroscopy. Our results show that the phenyl groups produce dramatic changes in the electronic structure of the fullerene system, including a lifting of the degeneracy of electronic states and a widening of the highest occupied molecular orbital–lowest unoccupied molecular orbital (HOMO–LUMO) bandgap, resulting in changes in the chemistry of the fullerene cage itself. The modification of the fullerene in this way also enhances the polarisation screening effect observed in fullerene systems. Adsorption at the Si(111)-(7×7) and Ag:Si(111)-(√3×√3)R30° surfaces is mediated by two different mechanisms, the former involving formation of covalent bonds, and the latter largely van der Waals in character. Despite the lack of a strong chemical interaction, however, a 0.9 ML coverage of (C₆H₅)₅C₆₀H on Ag:Si(111)-(√3×√3)R30° leads to a shift of the Si 2*p* core-level spectrum by ~200 meV to higher binding energy, suggesting that a positive interface dipole contributes to the adsorption energy of the fullerene at this surface.

DOI: [10.1103/PhysRevB.72.075426](https://doi.org/10.1103/PhysRevB.72.075426)

PACS number(s): 68.43.Bc, 71.20.Tx, 79.60.Dp, 61.10.Ht

I. INTRODUCTION

The discovery of fullerenes¹ was greeted with much excitement, generated by the belief that the new form of carbon could be exploited in the development of novel materials and electronic devices, drug delivery technology and nanoscale structures. Although some of the initial impetus in the field arguably faded somewhat, when very many practical or technological applications of C₆₀ (and its derivatives) did not immediately appear, a resurgence of interest in fullerene systems has recently been prompted by the fascinating (and highly cited) discovery of ferromagnetism in polymerized C₆₀ (Makarova *et al.*²). Furthermore, the exploitation of fullerenes as core elements of single molecule spectroscopy³ and manipulation^{4–7} experiments continues apace. A highly topical example is that of Yamachika *et al.*,⁸ who have shown that it is possible to controllably dope individual C₆₀ molecules placed, using an STM tip, above K atoms on a Ag surface.

A particularly attractive feature of the fullerene family of molecules is the ability to modify the molecular electronic structure via the introduction of various species, either inside the cage (yielding an endohedral-or incar fullerene),^{9–11} as a constituent of the cage (yielding a substitutionally doped molecule such as C₅₉N),¹² or attached to the cage (producing a functionalized fullerene).¹³ A wide variety of atoms (to date, around a third of the periodic table) can be encapsulated within a fullerene cage to yield endohedral fullerenes (e.g., N@C₆₀, La@C₈₂, Ce₂@C₈₀), in which the presence of the endohedral atom(s) can yield changes in the properties of the fullerene cage. Similarly, substitution of a different element for one or more of the constituent atoms of a fullerene cage can produce a system with an entirely different elec-

tronic structure. The addition of functional groups (for example, the phenyl groups discussed here) can introduce new chemistry to the fullerene system. Such modifications not only yield novel structural, electronic, and chemical behavior, but through the careful choice of functional species, this behavior is tunable, to some extent.

The addition of functional groups to the fullerene cage is of particular interest. Through the variation of the number, type and location of functional species, it is conceivable that the ordering of fullerenes within the bulk material and at surfaces may be tuned. The ability to vary the intermolecular separation within the material is of particular importance, as it facilitates the investigation of the interplay of conventional, delocalized band formation and electron correlation in fullerene systems. Controlled modification of the lattice constant of a doped-fullerene based molecular system changes the density of states at the Fermi level. This in turn has important implications for the modification of the critical temperature of superconducting fullerenes,^{14,15} although, once again, the importance of electron correlations should not be overlooked—the on-site Coulomb interaction in fullerene solids is much larger than the width of the conduction band. An important issue to address is whether cage functionalisation is an effective route to lattice constant variation. We must then ask not only how the presence of the functional groups affects molecular packing,¹⁶ but how the electronic structure of the fullerene molecule is modified. Moreover, there are a variety of surface science issues to be addressed: how do the phenyl groups affect adsorption, specifically molecular orientation, and is there any possibility of surface functionalization using functionalized fullerenes?

The functionalized fullerene of interest in this study, (C₆H₅)₅C₆₀H (Avent *et al.*¹³), is illustrated in Fig. 1. The five



FIG. 1. The bonding sites of the phenyl groups and hydrogen in $(C_6H_5)_5C_{60}H$ [after Avent *et al.* (Ref. 13)].

phenyl groups and single hydrogen cause rehybridization of six of the carbon centers in the fullerene cage, from sp^2 to sp^3 . This rehybridization results in a change in the double-single bond alternation pattern around the cage, affecting at least 20 carbon centers.

There are a variety of techniques available with which to probe the electronic structure of phenylated fullerene systems. Here we present the results of a study of $(C_6H_5)_5C_{60}H$ employing core-level (CL) and valence band (VB) photoemission (PES), and near-edge x-ray fine structure (NEXAFS) spectroscopy. We also compare the VB-PES data to results from density functional theory (DFT) calculations.

II. EXPERIMENTAL

The experimental work presented here was carried out at beamline 5u1 (Roper *et al.*,¹⁷ Mythen *et al.*¹⁸) of the Daresbury Laboratory Synchrotron Radiation Source. A 120 mm hemispherical analyzer from PSP¹⁹ was used for PES mea-

surements, and NEXAFS was carried out in total yield mode. Valence band spectra were acquired at the lower photon energy limit of the beamline, 60 eV (with energy resolution, ΔE , of ~ 140 meV, as measured from the Fermi edge broadening of the sample holder), Si $2p$ core-level spectra at 140 eV ($\Delta E \sim 160$ meV), and C $1s$ core-level spectra at 350 eV ($\Delta E \sim 250$ meV).

All measurements were carried out under ultrahigh vacuum (UHV) conditions, and the samples were prepared *in situ*. Si(111) substrates were thoroughly degassed using standard solvents and an ultrasonic bath before being loaded into the UHV system. This was followed by a period of degassing at 700 °C for a minimum of three hours.

The Si(111)-(7 \times 7) reconstruction was obtained through flash-annealing degassed Si(111) to 1200 °C, using direct heating. Preparation of Ag:Si(111)-($\sqrt{3}\times\sqrt{3}$)R30° was achieved by deposition of Ag onto the clean Si(111)-(7 \times 7) surface, held at 550 °C.

$(C_6H_5)_5C_{60}H$ was deposited from a K-cell at a temperature of ~ 350 °C. Multilayer coverages were obtained by deposition of material until the Si $2p$ peak was not visible in core-level measurements obtained at a photon energy of 140 eV. It has previously been shown, using STM,¹⁶ that annealing a multilayer sample at a temperature of ~ 300 °C produces a monolayer of $(C_6H_5)_5C_{60}H$ on the Si(111)-(7 \times 7) surface. Sub-monolayer coverages were estimated by comparison of the Si $2p$ to C $1s$ total-area ratio to that observed for the annealed monolayer.

III. RESULTS AND DISCUSSION

A. Bulk $(C_6H_5)_5C_{60}H$ / $(C_6H_5)_5C_{60}H$ thick films

The C $1s$ core-level spectrum of a thick $(C_6H_5)_5C_{60}H$ film is shown in Fig. 2, taken at both normal emission and 60° off normal emission. The figure also shows multivariate curve fits to the data, after the subtraction of a secondary electron background. The subtraction of a Shirley type background alone was not sufficient to eliminate all contributions due to

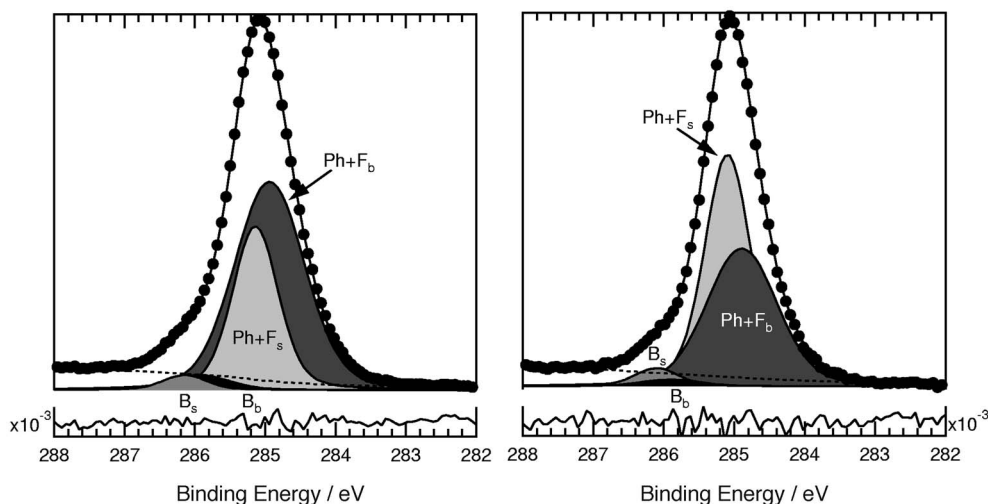


FIG. 2. C $1s$ core-level of bulk $(C_6H_5)_5C_{60}H$ taken at normal emission (a) and 60° off normal emission (b).

secondary electrons—a steadily increasing gradient remained. For this reason, the backgrounds shown here were obtained from the sum of a Shirley function and a polynomial of order three, the parameters for which were chosen to match the *gradient* of the raw data (rather than the raw intensity) far from the core-level. We found that this (admittedly somewhat involved) procedure produced a better fit than the Tougaard background subtraction method. Residuals associated with the core-level fitting process are shown below each fit. The *y* axis of each residual spectrum represents a range of $\pm 1 \times 10^{-3}$.

A minimum of three Voigt components were required to obtain a good fit to the C 1*s* spectra shown in Fig. 2. However, a physical justification of the characteristics of the components resulting from a three component fit is difficult. We expect discrete contributions to the C 1*s* core level from (at least) carbons of type sp^2 in the phenyl groups (phenyl—constituting 33% of all carbon in the molecule), sp^x where $2 < x < 3$ in the fullerene cage (fullerene—60%) and sp^3 which take part in bonding from the fullerene cage to the phenyl groups (bonding—7%). However, it is not likely that the separate contributions from phenyl and fullerene carbons may be resolved. We would, therefore, expect one component encompassing both the phenyl and fullerene contributions (Ph+F), and one from the bonding carbons (B). The latter would lie at around 0.8–1.2 eV higher binding energy, due to the shift associated with sp^2 and sp^3 hybrids.²⁰ A splitting of the order of 0.1 eV between the surface and bulk related C 1*s* components has previously been observed²¹ for C₆₀ films. This splitting arises from the differences in total final-state energy (due to core hole induced molecular polarisation), for molecules at the surface and in the bulk of a fullerene thin film.

Taking this difference in polarisation screening into consideration, we would expect two pairs of Ph+F and B components, with one pair shifted by at least 0.1 eV to higher binding energy. Four Voigt components were therefore used in a simultaneous fit to the normal and grazing emission spectra. The Lorentzian width of each of these components was set at 215 meV. This value is appreciably larger than the Lorentzian linewidth for the C 1*s* spectrum of bulk C₆₀ films, implying a shorter core-hole lifetime for phenylated C₆₀. However, recent work on carbon onions (Butenko *et al.*)²⁰ highlights that there may be other contributions to Lorentzian linewidth broadening (namely, contributions of phonons to the final state of the photoemission process, and effects due to the presence of different states in the bulk and at the surface of the material, which are not lifetime related). Gaussian widths and intensities were allowed to vary within physical limits. The initial positions of these components were chosen to yield components representing the Ph+F and B components in the bulk (*b*) and at the surface (*s*). However, the separation between bulk and surface pairs is of the order of the experimental resolution. To compensate for this, the positions were constrained such that the separation between Ph+F and B components at the surface matched that in the bulk, to within 10%. Otherwise, the positions were allowed to vary freely. In order to obtain a good fit to both spectra simultaneously, it was only necessary to allow the intensities and Gaussian widths of the components to differ

TABLE I. Fitting parameters for the curve fits shown in Fig. 2. The Lorentzian width (Γ_L) was fixed at 215 meV.

Component	Energy Γ_G		Total area/%		Partial area/%	
	/ eV	/ eV	NE	+60°	NE	+60°
Ph+F _{<i>b</i>}	285.14	1.06	60	44	94	96
B _{<i>b</i>}	+1.01	0.88	4	2	6	4
Ph+F _{<i>s</i>}	+0.20	0.64	33	50	92	93
B _{<i>s</i>}	+1.21	0.61	3	4	8	7

between normal and grazing emission: all other parameters were equivalent across both data sets. The parameters for the resulting fits are given in Table I.

There is considerable evidence to support the validity of this four-component fit. In moving from normal to grazing emission, surface sensitivity is increased; the fits show more surface character in the grazing emission spectrum. The relative intensities of the Ph+F and B components, both in the bulk and at the surface, are in excellent agreement with those expected (94% and 6%, respectively, compared to 93% and 7%). The Ph+F components are considerably broader than their corresponding B components. This is as expected, as the Ph+F component contains both sp^2 and sp^x ($2 < x < 3$) contributions, while the B component is due to sp^3 hybrids. It is also worthy of note that the bulk and surface Ph+F to B separations are identical, despite the 10% tolerance permitted during the fit.

From these fits, it is possible to conclude that the rehybridization of members of the fullerene cage in bonding to the phenyl groups produces a C 1*s* core-level shift of 1.0 eV. The local-field behavior due to polarization screening observed in C₆₀ systems²¹ is preserved, and its effect enhanced due to fullerene functionalization and the concomitant differences in molecular packing, in this case producing a shift of 0.2 eV between bulk and surface contributions. Furthermore, the bulk and surface Ph+F to B area ratios are very similar, and there is very little change in their values between the normal and grazing emission spectra. The lack of any significant change in the Ph+F:B surface ratio in particular indicates that (C₆H₅)₅C₆₀H does not occupy a preferred orientation at the surface of the multilayer. This is wholly consistent with observations from probe microscopy.¹⁶

The VB-PES and NEXAFS spectra of the thick (C₆H₅)₅C₆₀H film are presented in Fig. 3, along with those from a similar thick film of C₆₀ and theoretical valence bands for both molecules. The theoretical valence bands were produced by convolving orbital energies from B3LYP/6-31G* electronic-structure calculations with a Gaussian of width 0.35 eV. There is good agreement between these results and those obtained experimentally. The onset of the density of occupied states (valence band) of both molecules is comparable. The NEXAFS spectra show that the lowest unoccupied states of the fullerene are broadened and shifted due to the addition of the phenyl groups.

Although the onset of the valence band for both molecules is comparable, the NEXAFS measurements show that

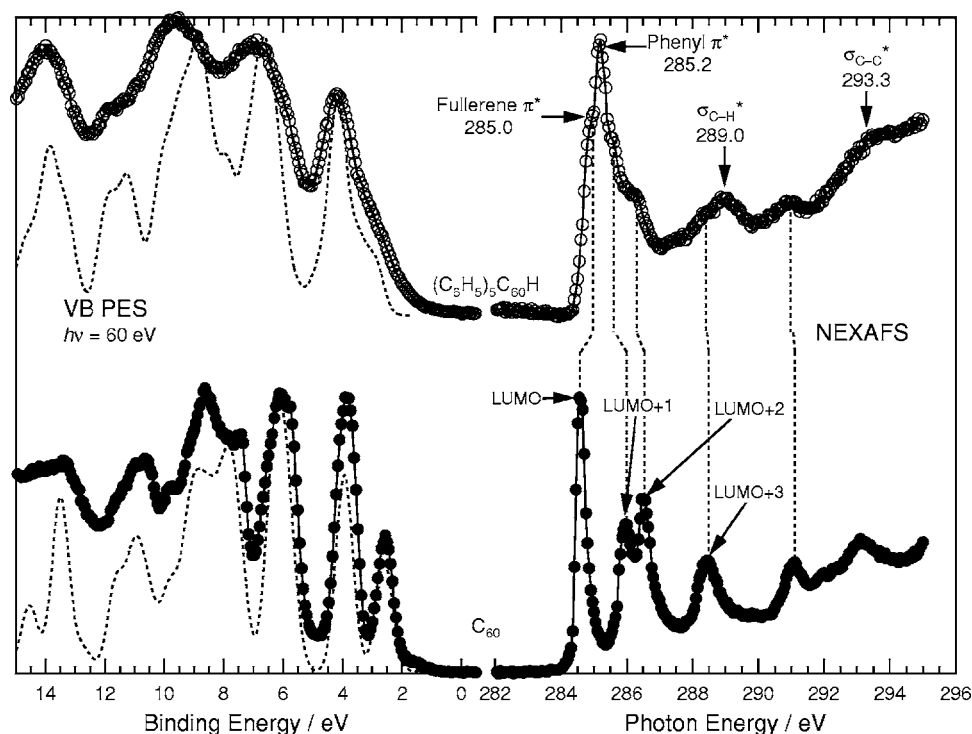


FIG. 3. Valence band photoemission and NEXAFS spectra for thick films of C_{60} (filled circles) and $(C_6H_5)_5C_{60}H$ (empty circles), along with valence bands from theory (dashed).

the edge of the unoccupied-state density is shifted by ~ 0.75 eV to higher energy in $(C_6H_5)_5C_{60}H$. As theoretical calculations (see Fig. 4 and Ref. 13) indicate that both the HOMO and LUMO are rather localised on the fullerene cage, we identify the shoulder at approximately 285 eV in the $(C_6H_5)_5C_{60}H$ NEXAFS data of Fig. 3 as arising from the fullerene cage. Following previous work^{22–24} the intense peak at 285.2 eV is attributed to the phenyl π^* -resonance. A second phenyl-derived resonance is located at 289.0 eV.^{22–24} Other resonances are largely fullerene-derived (see assignments in Fig. 4).

Taken together, the valence band, NEXAFS, and theoretical data shown in Figs. 3 and 4 illustrate that the phenyl groups make little direct contribution to the HOMO and LUMO in $(C_6H_5)_5C_{60}H$. The differences in the HOMO and

LUMO spatial distribution for $(C_6H_5)_5C_{60}H$ as compared to the parent fullerene molecule are due to phenyl-induced changes in the on-cage electronic structure. Furthermore—and of particular importance for the adsorption studies described below—one might imagine that bonding interactions between $(C_6H_5)_5C_{60}H$ and a surface are most likely to be driven by the cage-localized frontier orbitals rather than the phenyl groups.

No variation in the intensity of NEXAFS components was observed as a function of incidence angle. This gives little information concerning orientation or ordering within the multilayer—such a result could be expected in either an ordered or disordered case. A preferred orientation of the fullerene cage may be undetectable using NEXAFS due to its symmetry. If the $(C_6H_5)_5C_{60}H$ film were ordered, the phenyl

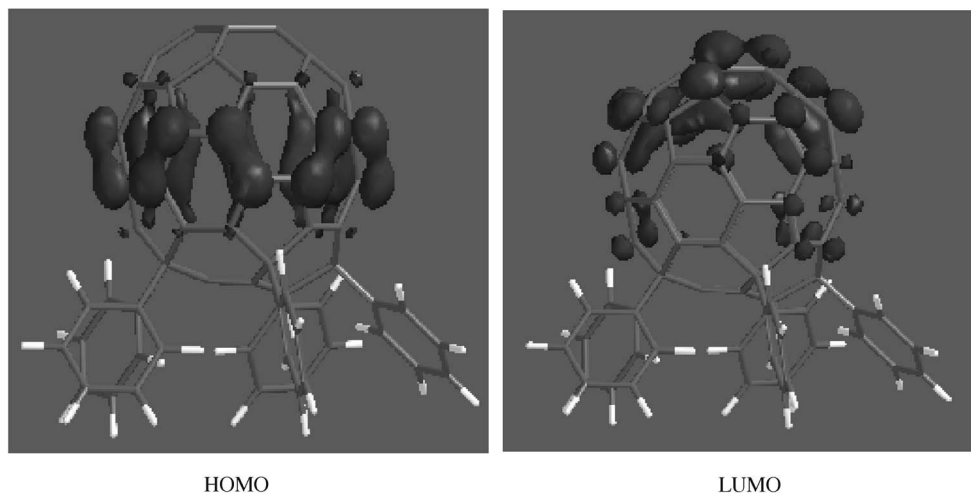


FIG. 4. The HOMO and LUMO of $(C_6H_5)_5C_{60}H$.

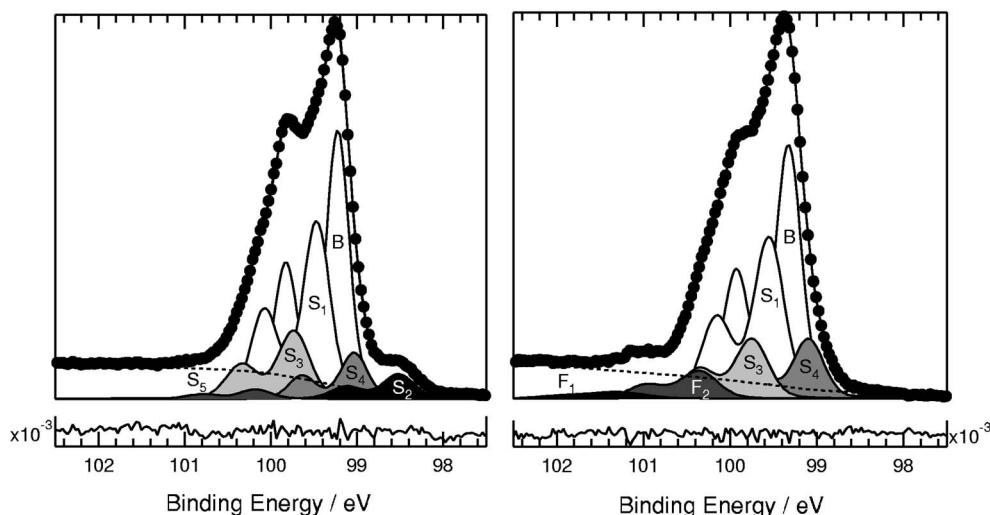


FIG. 5. Normal emission Si $2p$ core-levels of clean Si(111)-(7 \times 7) (a) and 0.7 ML $(C_6H_5)_5C_{60}H/Si(111)-(7 \times 7)$ (b), with curve fits. The parameters for the curve fits are given in Table II.

groups could still occupy a number of different orientations, by rotating to minimize both intermolecular and intramolecular phenyl-phenyl repulsions. All that can be concluded is that no interaction exists between molecules in the multilayer that causes alignment of the *phenyl* groups in a preferred orientation. This is consistent with scanning tunnelling microscopy studies of $(C_6H_5)_5C_{60}H$ films.¹⁶

B. $(C_6H_5)_5C_{60}H/Si(111)$

Si $2p$ core-levels for the clean Si(111)-(7 \times 7) surface and 0.7 ML of $(C_6H_5)_5C_{60}H/Si(111)$ sample are shown in Fig. 5, along with curve fits to the normal emission data. Normal and grazing emission C $1s$ spectra for the 0.7 ML coverage, both fitted, are presented in Fig. 6. Parameters for the Si $2p$ and C $1s$ curve fits are given in Tables II and III.

Seven components are present in the fit to the Si $2p$ core level for the clean surface—one bulk component, and six due

to surface core-level shifts (SCLS). The parameters for this fit compare well to those observed elsewhere.^{25,26} The components S_1 to S_5 have been assigned to the following features of the Si(111)-(7 \times 7) surface reconstruction:²⁶ pedestal atoms; rest atoms; adatoms; second-layer atoms; surface defects.

After deposition of $(C_6H_5)_5C_{60}H$, the rest-atom peak (S_3) is completely attenuated. All remaining surface components are broadened. This is to be expected with a sub-monolayer coverage of material, as an unsaturated monolayer results in a variety of chemical environments at the surface. In addition, a small peak [labeled F_2 in Fig. 5(b)] appears at an RBE of approximately 1.0 eV. A second very broad and weak component is observed at a RBE of ~ 2 eV; this component is labeled F_1 in Fig. 5(b). The 1.0 eV RBE peak, which is seen in the raw data as a small shoulder on the high binding energy side of the spectrum, arises from Si—C covalent

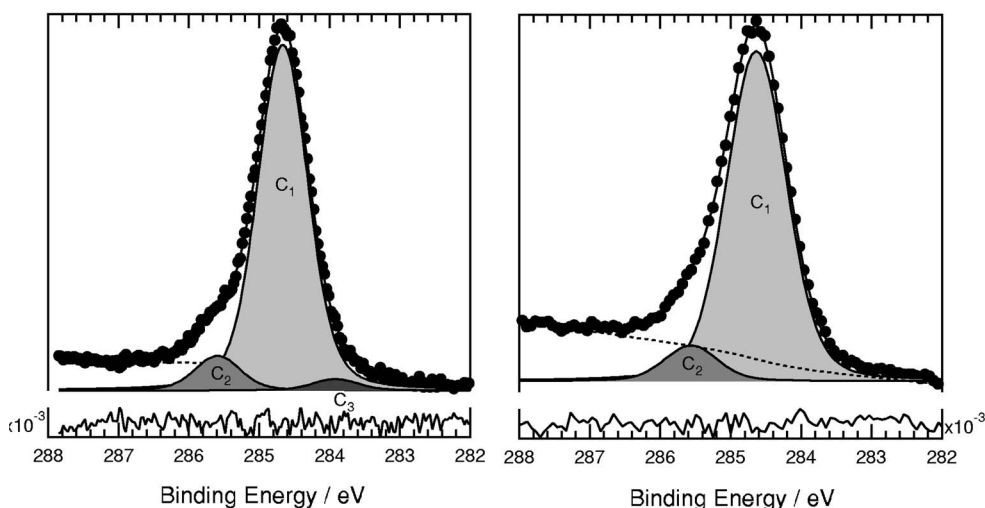


FIG. 6. Normal (a) and grazing emission (b) C $1s$ core levels for 0.7 ML $(C_6H_5)_5C_{60}H/Si(111)$, along with curve fits, the parameters for which are given in Table III.

TABLE II. Fitting parameters for Si $2p$ curve fits shown in Fig. 5.

	Clean Si(111)-(7×7)			0.7 ML (C ₆ H ₅) ₅ C ₆₀ H/Si(111)		
	Energy/eV	Γ _g /eV	Area/%	Energy/eV	Γ _g /eV	Area/%
Bulk	99.22	0.26	41	99.33	0.29	40
S ₁	+0.25	0.32	31	+0.23	0.37	30
S ₂	-0.71	0.38	5	—	—	—
S ₃	+0.51	0.38	13	+0.43	0.40	11
S ₄	-0.19	0.32	8	-0.23	0.37	11
S ₅	+0.96	0.38	2	—	—	—
F ₁	—	—	—	+1.95	0.65	2
F ₂	—	—	—	+1.03	0.45	6

Common parameters: Lorentzian width (Γ_L) 90 meV; Spin-orbit split 595 meV; Branching ratio 2.005.

bonds.^{27,28} A surface core-level shifted component with a RBE of $\sim +1$ eV has also been observed for Si—C bond formation following the adsorption of linear acenes on Si(111)-(7×7).²⁹ We note that one would not expect the intensity of the Si—C component at 1.0 eV RBE for a 0.7 ML (C₆H₅)₅C₆₀H coverage on Si(111)-(7×7) to match that observed for the C₆—Si(111)-(7×7) system as the bonding configurations, molecular orientation and packing density each differ strongly in both cases.

Three components are required to fit the normal emission C $1s$ spectrum. As before, we attribute the main peak to sp^x ($2 < x < 3$) carbons in the fullerene cage and sp^2 carbons in the phenyl groups. The presence of two similar chemical states account for its increased width, as compared to the other components. The component at +0.93 eV is due to sp^3 carbons involved in bonding between the fullerene cage and the phenyl groups. The shift of the third component (-0.75 eV) is comparable to that observed in the formation of Si—C bonds,³⁰ again suggesting a covalent interaction between (C₆H₅)₅C₆₀H and the substrate, and consistent with the discussion of the Si $2p$ core-level spectrum above. We note that while the component at -0.75 eV is extremely weak, its inclusion in the fit produces a lower χ^2 value and a more acceptable residual spectrum than is possible simply by using a two component fit and increasing the Gaussian (or Lorentzian) linewidth. Further evidence to support this assignment is found in the fact that the -0.75 eV component vanishes in the more surface sensitive grazing-emission spectrum. There is no significant change in the ratio of the C₁ to C₂ areas. This indicates that (C₆H₅)₅C₆₀H does not adsorb in such a way that all phenyl groups are directed either to-

wards or away from the surface, again consistent with investigations employing probe microscopy.¹⁶

C. (C₆H₅)₅C₆₀H/Ag:Si(111)

Figure 7 shows the Si $2p$ core-level of the Ag:Si(111)-(√3×√3)R30° surface before and after deposition of ~ 0.9 ML of (C₆H₅)₅C₆₀H. Considering the clean surface spectrum first, we note that the line shape is in very good agreement with previously published Si $2p$ core-level spectra of the Ag:Si(111)-(√3×√3)R30° reconstruction.³¹ However, as compared to the clean (7×7) surface, we observe a somewhat smaller binding energy shift (0.25 eV) of the entire spectrum than reported in previous work. For example, Tong *et al.*³² have observed a shift of the Si $2p$ spectrum by approximately 0.5 eV for the Ag:Si(111)-(√3×√3)R30° surface as compared to the clean Si(111)-(7×7) surface. We suggest that this discrepancy in absolute binding energy relates to a small amount of excess Ag present on the surface as a result of our preparation procedure.³³ As shown by Tong

TABLE III. Parameters for the C $1s$ curve fits shown in Fig. 6. The Lorentzian width was fixed at 215 meV.

	NE		+60°	
	Energy	Γ _g	Area	Area
C ₁	284.67	0.72	89	91
C ₂	+0.93	0.64	8	9
C ₃	-0.75	0.64	3	—

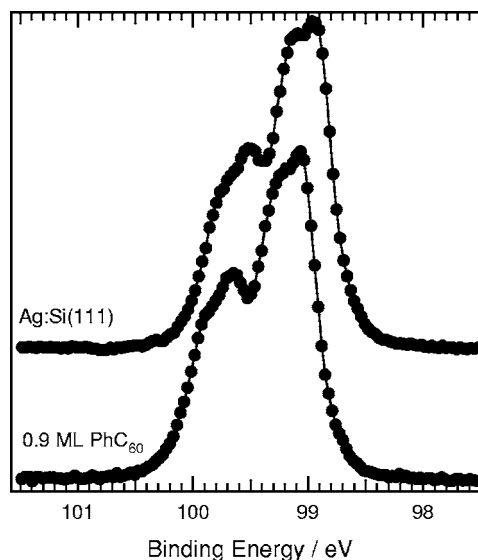


FIG. 7. Si $2p$ core levels of the clean Ag:Si(111) surface and of 0.9 ML (C₆H₅)₅C₆₀H/Ag:Si(111).

et al.,³² the presence of ~0.1 ML of additional Ag yields a binding energy shift of approximately 0.3 eV—much closer to the value we measure. It is worth noting that, following Hecht,³⁴ for the doping density of our samples (~10¹⁶ cm⁻³) and the photon flux used in the experiments, we can rule out surface photovoltaic effects as the origin of the shift.

Following adsorption of 0.9 ML of (C₆H₅)₅C₆₀H, although there is no significant change in the Si 2*p* line shape (as also previously observed for C₆₀ adsorption on Ag:Si(111)-(√3×√3)R30° (LeLay *et al.*³⁵), the core level undergoes a wholesale shift of 0.2 eV to higher binding energy. The lack of change in the Si 2*p* line shape strongly suggests that the interaction of the (C₆H₅)₅C₆₀H molecule with the underlying Ag-terminated Si(111) surface is extremely weak and lacks the covalent character that is a feature of fullerene adsorption on clean Si(111)-(7×7) surfaces.

The shift of the Si 2*p* peak to higher binding energy is intriguing. Hasegawa *et al.*³⁶ have proposed that C₆₀ acts as an electron acceptor when adsorbed on the Ag:Si(111)-(√3×√3)R30° reconstruction, compensating conduction electrons in the S₁ surface-state band^{32,37} of the substrate but, significantly, not promoting additional band bending. This scenario is consistent with the apparent lack of a Si 2*p* binding energy shift in the data published by LeLay *et al.*³⁵ However, as LeLay *et al.* do not explicitly comment on the binding energy of the Si 2*p* core-level, and in order to provide a direct comparison to the Si 2*p* data recorded for ~1 ML coverage of (C₆H₅)₅C₆₀H on Ag:Si(111)-(√3×√3)R30°, we have revisited the C₆₀ on Ag:Si(111)-(√3×√3)R30° system and studied the shift of the Si 2*p* core-level due to adsorption of the “parent” fullerene. We consistently find that, just as in the (C₆H₅)₅C₆₀H case, the Si 2*p* core-level shifts to 200 meV higher binding energy following the adsorption of 1 ML of C₆₀. In recent photoemission studies of pentacene adsorption at the Ag:Si(111)-(√3×√3)R30° surface, a shift of the Si 2*p* core-level peak by a few hundred meVs to higher binding energy has similarly been reported.³⁸

A shift of the Si 2*p* core-level to *higher* BE, in a simple band bending picture, would be consistent with a charge transfer from the adsorbed fullerenes to the underlying substrate—a somewhat surprising result given the propensity for charge transfer in the opposite direction for a very wide range of fullerene-surface systems. As noted above, the electrical transport data of Hasegawa *et al.*³⁶ have been interpreted in terms of charge transfer from the S₁ surface state band—a charge transfer that was suggested not to promote band bending. Importantly, however, in our recent experiments to probe Si 2*p* core-level shifts for the 1 ML C₆₀—Ag:Si(111)-(√3×√3)R30° system,³⁹ the Ag:Si(111)-(√3×√3)R30° surface was annealed prior to fullerene deposition so as to remove all excess Ag. The lack of excess Ag was verified via angle-resolved photoemission about the Γ-point of the second surface Brillouin zone. The S₁ surface state band, in our experiments, was, therefore, empty. Nevertheless, a Si 2*p* core-level shift of 200 meV to higher BE was observed following the adsorption of 1 ML of C₆₀.

Gensterblum *et al.*⁴⁰ carried out a careful and comprehensive study of the C₆₀/GeS(001) interface and found that the

substrate photoemission peaks shifted by 200 meV to higher BE. This result was rationalized in terms of delocalization of fractional fullerene charge over the substrate, giving rise to a positive interface dipole. Given our observation of an equivalent downward band-bending for both C₆₀ and (C₆H₅)₅C₆₀H monolayers on Ag:Si(111)-(√3×√3)R30°, it is clear that, while the fullerene-Ag:Si(111)-(√3×√3)R30° interaction is largely van der Waals in character, adsorption is accompanied by a similar molecule-to-substrate charge transfer or “delocalization” as observed for GeS(100) and involving the formation of a positive surface dipole. A change in work function for a semiconductor, as pointed out by Gensterblum *et al.*,⁴⁰ arises from two effects: a band-bending change and an interface dipole. Unfortunately, without a measurement of the work function of the sample (not carried out during this study), it is not possible to “disentangle” the band-bending and interface-dipole contributions and thus determine the magnitude of the dipole moment for each fullerene system.

It is nevertheless important to note that the observation of a positive binding energy shift for (C₆H₅)₅C₆₀H adsorption on Ag:Si(111)-(√3×√3)R30° is consistent with the bonding geometry proposed from STM measurements by Upward *et al.*¹⁶ The STM measurements have shown that (C₆H₅)₅C₆₀H molecules adopt an orientation on the Ag:Si(111)-(√3×√3)R30° surface where one phenyl group and a hexagonal face of the cage are in contact with the substrate. That is, the molecule effectively lies on its side rather than adopting a geometry in which the phenyl groups are pointed away from the surface or, conversely, where the unmodified part of the cage is separated from the surface by the phenyl groups. It is particularly interesting to realize that this “on-side” geometry will maximize the contact area of the equatorial belt of the molecule with the Ag-terminated Si(111) surface. As the molecular HOMO is localized around the equatorial belt, this provides a natural mechanism to promote molecule-to-substrate charge transfer (or delocalization of fullerene electrons) on the Ag:Si(111)-(√3×√3)R30° surface.

Coheur *et al.*⁴¹ have shown, using quantum chemical calculations, that each phenyl group donates 0.03e⁻±0.02e⁻ to the fullerene cage, with the H atom donating 0.22e⁻. The total excess charge on the unmodified (i.e., unfunctionalized) part of the cage was determined to be 0.176e⁻. The observation of identical 200 meV binding energy shifts for C₆₀ and (C₆H₅)₅C₆₀H adsorption, despite the lower areal density of (C₆H₅)₅C₆₀H,¹⁶ suggests that the dipole per molecule is greater for the phenylated fullerene monolayer, consistent with the excess charge density calculated by Coheur *et al.*⁴¹ We cannot, however, rule out the contribution of screening due to electrons donated from a very small coverage of “extraneous” Ag atoms to the S₁ band of the Ag:Si(111)-(√3×√3)R30° surface.

Finally, the C 1*s* core-level peak shifts from a binding energy of 284.8 eV for a 0.5 ML (C₆H₅)₅C₆₀H coverage to a value of 285.0 eV for a 1 ML coverage (the C 1*s* core-level binding energy for the bulk film is 285.1 eV). The similarity of the core-level binding energies for the monolayer and bulk films strongly suggests that image-charge screening due to the substrate does not play a key role in the final state of the

photoemission process. This observation indicates that while an interface dipole is present, the overall electronic structure of the $(\text{C}_6\text{H}_5)_5\text{C}_{60}\text{H}$ molecule is not strongly affected by adsorption on $\text{Ag}:\text{Si}(111)-(\sqrt{3}\times\sqrt{3})\text{R}30^\circ$.

IV. CONCLUSION

The modification of C_{60} through the addition of phenyl groups causes major alterations to the electronic structure of the fullerene, resulting in significant changes to the chemical behaviour of the system. In the frontier region, the phenyl groups make little direct contribution to the valence states—rather, they induce a lifting of the degeneracy in the electronic structure of the fullerene cage. In order to obtain good fits to the C 1s photoemission data acquired from thick films of $(\text{C}_6\text{H}_5)_5\text{C}_{60}\text{H}$, it is necessary to consider differences in polarization screening for molecules in surface- and bulk-like environments. There is considerable evidence to suggest a covalent interaction between $(\text{C}_6\text{H}_5)_5\text{C}_{60}\text{H}$ and the $\text{Si}(111)-(7\times 7)$ surface, as for C_{60} . The interaction of $(\text{C}_6\text{H}_5)_5\text{C}_{60}\text{H}$ with the $\text{Ag}:\text{Si}(111)-(\sqrt{3}\times\sqrt{3})\text{R}30^\circ$ surface, on the other hand, is much weaker, and largely van der Waals

in character. A shift of the Si 2p core level peak to higher binding energy, however, betrays the contribution of a small amount of molecule-substrate charge transfer (or delocalization of fullerene electrons across the substrate), as we have also observed for C_{60} adsorbed on the $\text{Ag}:\text{Si}(111)-(\sqrt{3}\times\sqrt{3})\text{R}30^\circ$ surface. Given the increasing use of the $\text{Ag}:\text{Si}(111)-(\sqrt{3}\times\sqrt{3})\text{R}30^\circ$ surface as a low energy substrate for the assembly of molecular monolayers and templates,⁴² the presence of a positive interface dipole should be taken into account in considering the overall interaction energy of adsorbed molecules on Ag-passivated Si(111). Future work will focus on determining the magnitude of this dipole.

ACKNOWLEDGMENTS

This work was funded by the Engineering and Physical Sciences Research Council (EP-SRC GR/01880/01). The authors would like to thank the following people: George Miller and Vin Dhanak, of the Daresbury SRS, for invaluable help and assistance during this beamtime, and for the provision of much-needed equipment; Karina Schulte, for very helpful discussions.

-
- ¹H. W. Kroto, J. R. Heath, S. C. O'Brien, R. F. Curl, and R. E. Smalley, *Nature* (London) **318**, 162 (1985).
- ²T. Makarova, B. Sundqvist, R. Hohne, P. Esquinazi, Y. Kopelevich, P. Scharff, V. Davydov, L. Kashevarova, and A. Rakhmanina, *Nature* (London) **413**, 716 (2001).
- ³J. Pascual, J. Gomez-Herrero, C. Rogero, A. Baro, D. Sanchez-Portal, E. Artacho, P. Ordejon, and J. Soler, *Chem. Phys. Lett.* **321**, 78 (2000).
- ⁴M. J. Butcher, J. W. Nolan, M. R. C. Hunt, P. H. Beton, L. Dunsch, P. Kuran, P. Georgi, and T. J. S. Dennis, *Phys. Rev. B* **67**, 125413 (2003).
- ⁵D. L. Keeling, M. J. Humphry, P. Moriarty, and P. H. Beton, *Chem. Phys. Lett.* **366**, 300 (2002).
- ⁶M. J. Butcher, F. H. Jones, P. Moriarty, P. H. Beton, K. Prassides, K. Kordatos, and N. Tagmatarchis, *Appl. Phys. Lett.* **75**, 1074 (1999).
- ⁷M. T. Cuberes, R. R. Schlittler, and J. K. Gimzewski, *Surf. Sci.* **371**, L231 (1997).
- ⁸R. Yamachika, M. Grobis, A. Wachowiak, and M. Crommie, *Science* **304**, 281 (2004).
- ⁹D. Bethune, R. Johnson, J. Salem, M. Devries, and C. Yannoni, *Nature* (London) **366**, 123 (1993).
- ¹⁰R. Johnson, M. Devries, J. Salem, D. Bethune, and C. Yannoni, *Nature* (London) **355**, 239 (1992).
- ¹¹Y. Chai, T. Guo, C. Jin, R. Hauffler, L. Chibante, J. Fure, L. Wang, J. Alford, and R. Smalley, *J. Phys. Chem.* **95**, 7564 (1991).
- ¹²J. Hummelen, B. Knight, J. Pavlovich, R. Gonzalez, and F. Wudl, *Science* **269**, 1554 (1995).
- ¹³A. G. Avent, P. R. Birkett, J. D. Crane, A. D. Darwish, G. J. Langley, H. W. Kroto, R. Taylor, and D. R. M. Walton, *J. Chem. Soc., Chem. Commun.* **1994**, 1463 (1994).
- ¹⁴S. Margadonna and K. Prassides, *J. Solid State Chem.* **168**, 639 (2002).
- ¹⁵A. Hebard, M. Rosseinsky, R. Haddon, D. Murphy, S. Glarum, T. Palstra, A. Ramirez, and A. Kortan, *Nature* (London) **350**, 600 (1991).
- ¹⁶M. D. Upward, P. Moriarty, P. H. Beton, P. R. Birkett, H. W. Kroto, D. R. M. Walton, and R. Taylor, *Surf. Sci.* **405**, L526 (1998).
- ¹⁷M. Roper, G. van der Laan, H. Durr, E. Dudzik, S. Collins, M. Miller, and S. Thompson, *Nucl. Instrum. Methods Phys. Res. A* **467**, 1101 (2001).
- ¹⁸C. S. Mythen, G. Vanderlaan, and H. A. Padmore, *Rev. Sci. Instrum.* **63**, 1313 (1992).
- ¹⁹*Psp vacuum technology*, <http://www.pspvacuum.com/>.
- ²⁰Yu. V. Butenko, S. Krishnamurthy, A. K. Chakraborty, V. L. Kuznetsov, V. R. Dhanak, M. R. C. Hunt, and L. Siller, *Phys. Rev. B* **71**, 075420 (2005).
- ²¹E. Rotenberg, C. Enkvist, P. A. Bruhwiler, A. J. Maxwell, and N. Martensson, *Phys. Rev. B* **54**, R5279 (1996).
- ²²D. Wacker, K. Weiss, U. Kazmaier, and C. Woll, *Langmuir* **13**, 6689 (1997).
- ²³C. Mainka, P. Bagus, A. Schertel, T. Strunskus, M. Grunze, and C. Woll, *Surf. Sci.* **341**, L1055 (1995).
- ²⁴M. Yang, M. Xi, H. Yuan, B. Bent, P. Stevens, and J. White, *Surf. Sci.* **341**, 9 (1995).
- ²⁵G. LeLay, M. Gotherid, T. M. Grehk, M. Bjorkquist, U. O. Karlsson, and V. Y. Aristov, *Phys. Rev. B* **50**, 14277 (1994).
- ²⁶C. J. Karlsson, E. Landemark, Y. C. Chao, and R. I. G. Uhrberg, *Phys. Rev. B* **50**, R5767 (1994).
- ²⁷J. N. O'Shea, M. A. Phillips, M. D. R. Taylor, P. H. Beton, P. Moriarty, M. Kanai, T. J. S. Dennis, V. R. Dhanak, S. Patel, and N. Poolton, *J. Chem. Phys.* **119**, 13046 (2003).
- ²⁸K. Sakamoto, M. Harada, D. Kondo, A. Kimura, A. Kakizaki, and S. Suto, *Phys. Rev. B* **58**, 13951 (1998).
- ²⁹G. Hughes, D. Carty, and A. A. Cafolla, *Surf. Sci.* **582**, 90

- (2005).
- ³⁰M. de Seta, N. Tomozeiu, D. Sanvitto, and F. Evangelisti, *Surf. Sci.* **460**, 203 (2000).
- ³¹G. LeLay, *Surf. Rev. Lett.* **4**, 287 (1997).
- ³²X. Tong, C. S. Jiang, and S. Hasegawa, *Phys. Rev. B* **57**, 9015 (1998).
- ³³R. I. G. Uhrberg, H. M. Zhang, T. Balasubramanian, E. Landemark, and H. W. Yeom, *Phys. Rev. B* **65**, 081305(R) (2002).
- ³⁴M. H. Hecht, *Phys. Rev. B* **41**, 7918 (1990).
- ³⁵G. LeLay, M. Gothelid, V. Y. Aristov, A. Cricenti, M. C. Hakanson, C. Giammichele, P. Perfetti, J. Avila, and M. C. Asensio, *Surf. Sci.* **377**, 1061 (1997).
- ³⁶S. Hasegawa, K. Tsuchie, K. Toriyama, X. Tong, and T. Nagao, *Appl. Surf. Sci.* **162**, 42 (2000).
- ³⁷L. S. O. Johansson, E. Landemark, C. J. Karlsson, and R. I. G. Uhrberg, *Phys. Rev. Lett.* **63**, 2092 (1989).
- ³⁸G. Hughes, D. Carty, O. McDonald, and A. Cafolla, *Surf. Sci.* **580**, 167 (2005).
- ³⁹L. Wang, K. Schulte, J. Hayton, V. Dhanak, G. Miller, and P. Moriarty (in preparation).
- ⁴⁰G. Gensterblum, K. Hevesi, B.-Y. Han, L.-M. Yu, J.-J. Pireaux, P. A. Thiry, R. Caudano, A. A. Lucas, D. Bernaerts, S. Amelinckx, G. Vantendeloo, G. Bendele, T. Buslaps, R. L. Johnson, M. Foss, R. Feidenhansl, and G. le Lay, *Phys. Rev. B* **50**, 11981 (1994).
- ⁴¹P.-F. Coheur, J. Cornil, D. A. dos Santos, P. R. Birkett, J. Lievin, J. L. Bredas, D. R. M. Walton, R. Taylor, H. W. Kroto, and R. Colin, *J. Chem. Phys.* **112**, 8555 (2000).
- ⁴²J. A. Theobald, N. S. Oxtoby, M. A. Phillips, N. R. Champness, and P. H. Beton, *Nature (London)* **424**, 1029 (2003).